AUSTRALIAN JOURNAL OF BASIC AND APPLIED SCIENCES

ISSN:1991-8178 EISSN: 2309-8414
Journal home page: www.ajbasweb.com

3D Modeling of Interaction Jets With A Compressible Transverse Flow

Djamel Cherrared

Faculty of Mechanical and Process Engineering, Houari Boumedienne University B.P. 32 El Alia, Algiers, Algeria

Address For Correspondence:
Faculty of Mechanical and Process Engineering, Houari Boumedienne University B.P. 32 El Alia, Algiers, Algeria
Phone and fax numbers: 00 (213) 21 20 77 65. E-mail address: cherrared_d@yahoo.fr

ARTICLE INFO

Article history:
Received 26 August 2016
Accepted 10 October 2016
Published 18 October 2016

Keywords:
Compressible flow, film cooling, gas turbine blade, jet, modelisation, turbulence.

ABSTRACT

A numerical three-dimensional study of the interaction of a row of discrete jets in a wall with a transversal compressible flow (Mach number Ma=0.72), for small injection rate (R=0.6) is performed. Its importance is in the application of cooling the turbojets blades. The computational domain is chosen to be a periodic domain. The problem considered is a single inclined row of round subsonic jets exhausting through a large flat plate into a compressible boundary layer to a cross flow. Favre-averaged Navier-Stokes equations were solved using a finite volume method. Turbulence closure was achieved using an explicit algebraic stress model (EASM). The accuracy of the method is assessed by comparison with available experimental results. A reasonable quantitative agreement was obtained for the flow field. Results for the temperature field are also presented. The non-linear model (EASM) gives a reasonable prediction.

INTRODUCTION

It is well known from thermodynamic analysis that the performance of a gas turbine is strongly influenced by the inlet temperatures. Modern gas turbine engines are designed to operate at inlet temperatures of 1800-2200 °K which are far beyond the allowable metal temperatures. Thus, to maintain acceptable life and safety standards, the structural elements must be protected against the severe thermal environment. This calls for an efficient system by adding an efficient cooling system. One such cooling technique currently used for high temperature turbines, is film-cooling.

The present paper aims to contribute to the development of a prediction method for the simulation and to the understanding of the cooling behaviour. The application of computational fluids dynamics to film cooling problem is assessed in this study. Results are presented in terms of temperature contours and calculation of velocity in the flow field.

A considerable effort has been devoted to understanding the coolant film behavior and its interaction with the mainstream flow. The impact of the jet hole arrangement, the blowing ratio, and the density ratio was investigated by Baldauf *et al*. (1999). Until recently, the only possible means of numerically simulating such a flow has been through solving the Reynolds-averaged Navier–Stokes (RANS) equations coupled with an appropriate turbulence model (Hoda and Acharya, 2000). These turbulence models, however, usually fail to predict accurately the flow field due to the presence of the strong curvature of the streamlines as well as the reverse flow occurring downstream of the jet exit (Hahn and Choi, 1997).

Baherie *et al*. (2008) reported a comparative-numerical investigation on film cooling from a row of simple and compound-angle holes injected at 35° on a flat plate with four film cooling configurations. The mathematical film-cooling model consists of the RANS (Reynolds Averaged Navier–Stokes equations), the energy equation and the standard k–ε model with standard logarithmic wall function. All simulations are at fixed density ratio of 1.6 with an injection rate of 1.25. It has been shown that the film cooling effectiveness by

To Cite This Article: Djamel Cherrared., 3D Modeling of Interaction Jets With A Compressible Transverse Flow. ***Aust. J. Basic & Appl. Sci.,*** *10(15): 1-9, 2016*

trenched shaped holes is higher than all other configurations both in spanwise and streamwise especially downstream of the injection. Also, a trenched compound angle injection shaped hole produces much higher film cooling protection than the other configurations.

Bayraktar and Yılmaz (2011) investigated numerically a lot of parameters that affect the film cooling performance. Five different inclination angles (α=30°, 45°, 60°, 75° and 90°), four blowing ratios (R = 0.2, 0.5, 1.0, 2.0), two different nozzle geometries, namely, circular and square shaped have been considered for multiple nozzles. Renormalized (RNG) k–ε turbulence model was used as turbulence closure. The performance of RNG k–ε turbulence model was tested by comparing with available experimental data found in the literature and it has observed that both results are in good agreement. They that maximum cooling efficiency is obtained at inclination angle of 30° and the blowing ratio of 2.0. They noted that circular shaped nozzle provides more effective cooled surface than square shaped nozzles. Their papers show also the dependence of the cooling efficiency to the one of the most important vortex structure of counter-rotating vortex pair.

To gain more knowledge about the vortex dynamics, the influence of flow parameters on the flow field, and the turbulence structure up and downstream of the jet/crossflow interaction region, Tyagi and Acharya (2003), Guo *et al*. (2006) apply a more precise turbulence description such as large-eddy simulation (LES) to investigate the interaction of the jet flow with the cross-flow. However, the LES requires also very large computer memory and processing time. In order to combine simplicity, generality and efficiency, the present work study uses the explicit algebraic stress models (EASM) of Rumsey *et al*. (2000). The EASM is based on approach originally developed by Pope (1975) in two-dimensional structure, extended by Gatski and Speziale (1993) to three-dimensional flows.

The EASM approach allows for the inclusion of the stress anisotropies and rotation effects and takes into account the dissipation rate anisotropies. These models (EASM) have shown that is a practicable approximation for a various range of complex engineering applications such as turbomachinery problems, aircraft turbines, etc.

In this study, we have studied the behavior of EASM model of Rumsey *et al*. (2000). The performances and accuracy of this model is estimated in comparison with the experiment results of Dizene *et al*. (2000).

The test case studied here represents film cooling of a flat plate using a single row of inclined circle jets as an angle of 45° issued in crossflow. This test case was studied experimentally in detail by Dizene *et al*. (2000). The geometrical configuration is presented in Figure 1. Dizene and al. (2000) showed that the phenomenon is periodic, no interaction between the jets. Further, one symmetry is observed in the center of the jet at the axis Z/D in the results of Dizene *et al*. (2000). Thereby, the computational domain is chosen to be a periodic module and the study domain is shown in Figure 1. The experiments are carried out for cross flow Mach number of 0.72 and the injection rate R=0.6. The problem considered is a single inclined row of round subsonic jets exhausting through a large flat plate into a compressible boundary layer of a cross flow.

The figure 1 takes into account the physics of the aerodynamic/film cooling interaction problem without the added complexity of the blade curvature. In the present work, the mechanisms of the interaction process are assessed by a study of the characteristics of the flow field and of the thermal field. Several results are presented in this study highlighting the interaction of the jet with the compressible cross-flow to contribute to the development of a prediction method for the simulation and to the understanding of the cooling behaviour.

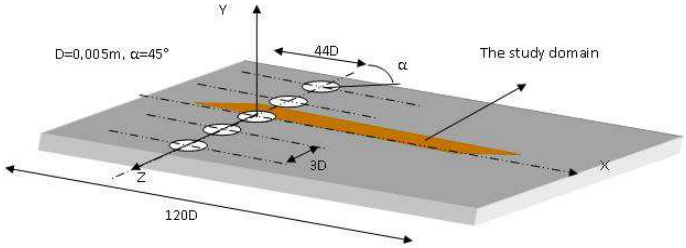

Fig. 1: Experimental test facilities (Dizene *et al*. 2000)

The Description Problemand The Computational Model:

The flow configuration studied is a round inclined turbulent jet discharging into a cross-flow in a rectangular tunnel. A schematic drawing of the free jet coordinate system is given in Figure 2.

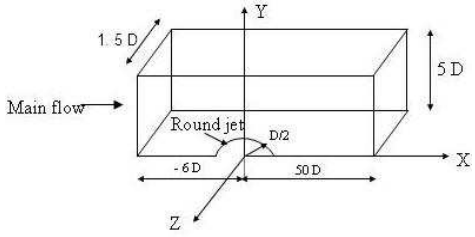

Fig. 2: Flow configuration, computational domain and coordinate system (Symmetric plane Z = 0)

The Favre-averaged equations governing the fluid for mass, momentum and energy conservation transport are given below:

$$\frac{\partial}{\partial x_i}\left(\bar{\rho}\tilde{U}_i\right)=0 \tag{1}$$

$$\frac{\partial}{\partial x_i}\left(\bar{\rho}\tilde{U}_i\tilde{U}_j\right)=-\frac{\partial \bar{P}}{\partial x_i}+\frac{\partial}{\partial x_i}\left(\bar{\tau}_{ij}-\overline{\rho u_i u_j}\right) \tag{2}$$

$$\frac{\partial}{\partial x_i}\left(\bar{\rho}\tilde{U}_i\tilde{T}_j\right)=\frac{\tilde{U}_i}{C_p}\frac{\partial \bar{P}}{\partial x_i}+\frac{\partial}{\partial x_i}\left(\frac{\mu}{Pr}\frac{\partial \tilde{T}}{\partial x_i}\right)+\frac{\overline{\tau_{ij}}\frac{\partial U_j}{\partial x_i}}{C_p}+\frac{\partial\left(-\overline{\rho u_i \theta}\right)}{\partial x_i} \tag{3}$$

The viscous stress tensor is given by:

$$\bar{\tau}_{ij}=\overline{2\mu\left(S_{ij}-\frac{1}{3}S_{kk}\delta_{ij}\right)}\approx 2\bar{\mu}\left(\tilde{S}_{ij}-\frac{1}{3}\tilde{S}_{kk}\delta_{ij}\right) \tag{4}$$

$\bar{\mu}$ the mean molecular velocity, P_r the Prandtl number $(P_r=0.7)$.

Algebraic Stress Model (ASM) originates from Reynolds stresses closures under assumptions about the convective and diffusive terms (see, for example, Gatski and Speziale, 1993). The result is an implicit algebraic equation for anisotropic Reynolds stresses b_{ij}. Since such a representation is implicit, the numerical robustness of its solution can be questionable. The EASM used here replaces this implicit relation with a polynomial expansion in a tensor basis. In addition, a linear pressure-strain rate correlation model and an isotropic dissipation rate are assumed. In the present study, the ASM model version of Rumsey *et al*. (2000) was implemented and used with the standard k-ε model version.

$$-\overline{\rho u_i u_j}=-\frac{2}{3}\bar{\rho}K\delta+2\mu_t^*\left\{\left(\tilde{S}_{ij}-\frac{1}{3}\tilde{S}_{kk}\delta_{ij}\right)+\beta_2\frac{K}{\varepsilon}\left(\tilde{S}_{ik}\tilde{\omega}_{kj}+\tilde{S}_{jk}\tilde{\omega}_{ki}\right)-2\beta_3\frac{K}{\varepsilon}\left(\tilde{S}_{ik}\tilde{S}_{kj}-\frac{1}{3}\tilde{S}_{kl}\tilde{S}_{kl}\delta_{ij}\right)\right\} \tag{5}$$

Where $\mu_t^*=\bar{\rho}C_\mu^*\frac{K^2}{\varepsilon}$, $C_\mu^*=\frac{3\left(1+\eta^2\right)+0.2\left(\eta^6+\varsigma^6\right)}{3+\eta^2+6\varsigma^2\eta^2+6\varsigma^2+\eta^6+\varsigma^6}a_4a_1$, $\eta=\beta_3\frac{K}{\varepsilon}\left(\tilde{S}_{ij}\tilde{S}_{ij}\right)^{1/2}$, $\varsigma=\beta_2\frac{K}{\varepsilon}\left(\tilde{\omega}_{ij}\tilde{\omega}_{ij}\right)^{1/2}$

The EASM used here is then the version described by Rumsey *et al*. (2000).The explicit algebraic stress model is an extension of the Gatski and Speziale (1993) model. β_1, β_2 and β_3 are given by:

$$\gamma_0^2\beta_1^3-\frac{\gamma_0\gamma_1}{\eta_1^2(K/\varepsilon)}\beta_1^2+\frac{1}{4\eta_1^4(K/\varepsilon)^2}\left[\gamma_1^2-2(K/\varepsilon)^2\gamma_0a_1\eta_1^2-2\eta_1^2(K/\varepsilon)^2\left(\frac{a_3^2}{3}-\Re^2a_2^2\right)\right]\beta_1+\frac{1}{4\eta_1^6(K/\varepsilon)}\left(\gamma_1a_1\eta_1^2\right)=0 \tag{6}$$

$$\begin{aligned}\beta_2&=a_2a_4\\ \beta_3&=a_3a_4\end{aligned} \tag{7}$$

With

$$a_1=\left(\frac{4}{3}-C_2\right)\frac{1}{2},\quad a_2=\left(2-C_4\right)\frac{1}{2},a_3=\left(2-C_3\right)\frac{1}{2},\quad a_4=g$$

Where g is variable quantity given by equation bellow:

$$g=\left(\gamma_0\frac{G}{\varepsilon}+\gamma_1\right)^{-1}=\left(-2\gamma_0\beta_1\eta_1^2(K/\varepsilon)+\gamma_1\right)^{-1},\ \gamma_0=1.9,\ \gamma_1=0.7,\ \Re^2=\frac{\xi_1^2}{\eta_1^2}=\frac{\tilde{\omega}_{ij}\tilde{\omega}_{ij}}{\tilde{S}_{ij}\tilde{S}_{ij}}$$

For the Speziale *et al*. (1991), these coefficients are:

$C_3=1.25, C_4=0.4$, with $C_2=\frac{4}{5}-1.5\Pi_b^{1/2}$

Where $\prod_b=b_{ij}b_{ij}$ and the anisotropy of the Reynolds stress b_{ij} is defined as:

$$b_{ij}=\frac{\overline{u_iu_j}-\frac{2}{3}K\delta_{ij}}{2K}$$

It is easily shown that the production to dissipation rate ratio is given by:

$$\frac{G}{\varepsilon}=-2\left\{b\tilde{S}\right\}(K/\varepsilon),\left\{b\tilde{S}\right\}=\beta_1\eta_1^2$$

The proper choice for β_1 is the minimum real root of Eq. (6) (Jongen and Gatski, 1998). The following equations are used for the solution of the standard K-ε model.

$$\frac{\partial}{\partial x_i}\left(\bar{\rho}\tilde{U}_iK\right)=\frac{\partial}{\partial x_i}\left((\mu+\frac{\mu_t}{\sigma_K})\frac{\partial K}{\partial x_i}\right)+G-\bar{\rho}\varepsilon \tag{8}$$

$$\frac{\partial}{\partial x_i}\left(\bar{\rho}\tilde{U}_i\varepsilon\right)=\frac{\partial}{\partial x_i}\left((\mu+\frac{\mu_t}{\sigma_\varepsilon})\frac{\partial \varepsilon}{\partial x_i}\right)+C_{\varepsilon1}\frac{\varepsilon}{K}G-C_{\varepsilon2}\bar{\rho}\frac{\varepsilon^2}{K} \tag{9}$$

Where $G = -\overline{\rho u_i u_j}\frac{\partial \tilde{U}_i}{\partial x_j}$, $C_\mu = 0.09$, $C_{\varepsilon 1} = 1.44$, $C_{\varepsilon 2} = 1.92$, $\sigma_k = 1.0$ and $\sigma_\varepsilon = 1.3$

The flow field is completely defined by means of the perfect gas law: $\overline{P} = \overline{\rho} r \tilde{T}$. An isotropic simple eddy diffusivity model based on the Boussinesq approximation is used to provide closure for the turbulent heat flux terms.

$$-\overline{\rho u_i \theta} = \frac{\mu_t}{Pr_t}\frac{\partial \tilde{T}}{\partial x_i} \quad (10)$$

Where the turbulent Prandtl number Pr_t is 0.9, G is the production term in K-ε equation.

The Numerical Technique:

The computational methodology used for simulation of the flow is based on the finite volume method. We have developed a computer code for modelise numerically the three-dimensional turbulent flows with compressible fluids. In the computer code, the Semi-Implicit Method for Pressure-Linked Equations (SIMPLE) of Patankar (1980) is used to handle the pressure-velocity coupling. The SIMPLE algorithm used in the pressure correction equation resolution is a modified and an adapted version for the compressible flow. Diffusion terms appearing in the transport equations for momentum and turbulence parameters are discretized using second-order central differencing. The Power-Law Differencing Scheme (PLDS) of Patankar (1980) is taken to treat the convection terms. An algorithm based on TDMA (Tri-Diagonal Matrix Algorithm) is used for solving the equations. For fully developed flows, the solver was iterated until a fully converged solution was attained. Non uniform grids were generated, and grid refinement close to the wall and injection zone was applied.

The Boundary Conditions:

The accuracy of the numerical solution depends on the boundary conditions and the way that these are integrated within the numerical model. In our case, there are four kinds of boundary conditions: flow and jet inlet conditions, flow outlet conditions, symmetry conditions and wall boundary conditions. All the variables must be specified at the inflow boundary and the jet exit and eventually taken from the measurement values.

Inlet flow (X/D=- 6)

The boundary layer	$\tilde{U} = \tilde{U}_e(Y/\delta)^{1/7}$, $(\tilde{T}-\tilde{T}_e)/(\tilde{T}_w-\tilde{T}_e) = (Y/\delta_t)^{1/5}$, $\tilde{V}=0$, $\tilde{W}=0$, $K = C_\mu^{-0.5} lm(\partial\tilde{U}/\partial Y)^2$, $\varepsilon = K^{3/2}/(C_\mu^{-3/4} 0.09\, lm)$
The external flow	$\tilde{U} = \tilde{U}_e$, $\tilde{U}_e = 248\ m/s$, $\tilde{T} = \tilde{T}e, \tilde{T}e = 262^\circ K$, $\tilde{V}=0$, $\tilde{W}=0$, $K = 1.5\overline{u^2}$, $\varepsilon = K^{3/2}/(C_\mu^{-3/4} 0.09\delta)$

The choice of K is based on $\sqrt{u^2}/\tilde{U}_e = 0.02$, $lm = \min(\chi y, 0.09\delta)$ and $\chi = 0.41$ is the Von Karman constant

Inlet jet (X/D=0)

The penetration velocity of the jet	$R = \overline{\rho}_j \tilde{V}_j / \overline{\rho}_e \tilde{U}_e \rightarrow \tilde{V}_j = \overline{\rho}_e \tilde{U}_e R / \overline{\rho}_j$, $R = 0.6$
The three velocity components of the jet	$\tilde{U} = \tilde{V}_j \cos(\alpha)$, $\tilde{V} = \tilde{V}_j \sin(\alpha)$, $\tilde{W} = 0$, $\alpha = 45°$
the conditions for K-ε and the temperature	$K = 0.005 \cdot \tilde{U}_e$, $\varepsilon = K^{3/2}/(0.3 \cdot 0.5 \cdot D)$, $\tilde{T} = \tilde{T}_j$, $\tilde{T}_j = 327^\circ K$

Outlet flow (X/D=50)

The outlet boundary conditions are imposed at a fully developed flow section. The Newman boundary conditions are applied in this section.

Symmetry conditions:

A null gradient for all the physical quantities governed by a differential equation of transport.

All these conditions are summarized in Figure 3.

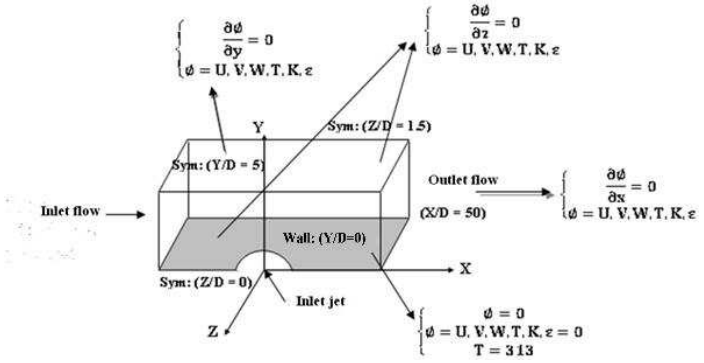

Fig. 3: Boundary conditions

Wall boundary condition (Y/D=0):

The classical no-slip boundary conditions are assured at the wall. We imposed a fixed value of temperature $\tilde{T}_w = 313^\circ$ K. The well-known wall function for the velocity and temperature are employed to provide the all boundary treatment. Assuming a two-layer structure of the boundary layer, the wall functions have the following forms:

$$U^+ = \begin{cases} y^+ & \text{if} \quad y^+ < 11.63 \\ \ln(Ey^+)/\chi & \text{otherwise} \end{cases} \tag{11}$$

$$T^+ = \Pr y^+ \quad \text{if} \quad y^+ < 11.63 \tag{12}$$

$$T^+ = \Pr_t \left(U^+ + f(pr/pr_t)\right) \quad \text{otherwise}$$

Where $y^+ = \overline{\rho} C_\mu^{0.25} K_p^{0.5} y_p / \mu$

y_p is the normal distance from the wall.

P: refers to the first control volume from the wall. In these equations, the constants χ and E are 0.41 and 9.79, respectively. The diffusive flux of turbulence kinetic energy is zero at the wall, and the near wall values of the production rate G_p and the dissipation rate ε_p are determined from (Launder and Spalding, 1974)

$$G_p = \tau_w \tilde{U}_p / y_p \text{ where } \tau_w = -\tilde{U}_p \chi \mu \, y^+ / y_p \ln(Ey^+), \quad \varepsilon_p = C_\mu{}^{0.75} K_p{}^{1.5} U^+ / y_p \tag{13}$$

RESULTS AND DISCUSSION

The computational domain of interest is shown in figure 1, where (X, Y, Z) = (0, 0, 0) refers to the center of a jet at the jet exit. The inlet boundary conditions for the cross-flow are obtained from measured data for a fully developed boundary-layer flow over a flat plate (Dizene *et al*., 2000). The computational domain in y direction extends from Y/D = 0 to Y/D = 5 planes. The mean velocity field and the mean temperature field are compared with available experimental results. The velocity is nondimensionalized with respect to the external streamwise velocity $\tilde{U}_e$. The temperature is represented by the nondimensional local temperature in film. Both the measured data and the previous numerical results show that the jet and the cross-flow interact strongly with each other at the jet exit so that the influence is propagated toward the upstream direction of the jet. Consequently, the jet bending can be seen to start already at the pipe exit.

Some details of the jet interaction with the main flow near the injection are illustrated in Figure 4 by the velocity vectors at X/D = 0, 0.5, 1 and 2 in the transverse plane (Y, Z). They show the development of large vortex structure, where a pair of vortex is clearly established at X/D = 0.5: this in counter rotating vortices which seems to be centred at Z/D = 0.5, Y/D = 0.1 and to move away of the wall towards the jet axis at position (X/D = 4) . The vortex should having lost its strength X/D = 1 so its size decreases. This behaviour implies the individual character of each jet in compressible flow. The accurate vortex location and its motion has not been invistigated in the study of Dizene *et al*. (2000) in the experimental results.

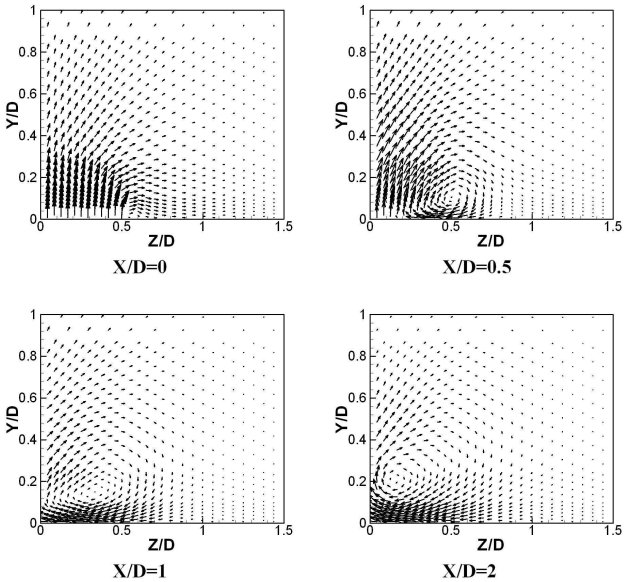

Fig. 4: Computed velocity vectors at vertical planes along Z/D direction by the EASM.

Further information of the accurate prediction of jet penetration can be seen in Figure 5 (at Z/D=0). This figure shows the existence of an overpressure upstream of orifice and a depression downstream. This pressure difference provides the force necessary to deform the jet. Thus, the jet curves itself and tends to align itself in the transverse flow direction.

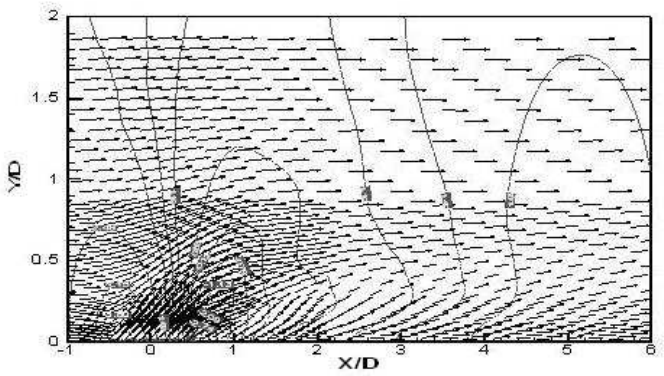

Fig. 5: Computed velocity vectors and constant pressure contours profiles in center plane

The Figure 6 shows the velocity vectors ploted from $\tilde{U}$ and $\tilde{W}$ in the lateral plane (X, Z) at $Y \approx 0$. The results show the bypassing of jet by the main flow until Z/D = 0.75. We notice the deceleration of the jet in upstream and the acceleration in downstream. We do not see any inverse flow region downstream of the injection region. This result has also been observed by Dizene *et al*. (2000) when comparing normal and oblique configuration jet flows. He noticed that inverse flow region behind the normal jet seems to be desapeared behind the oblique jet.

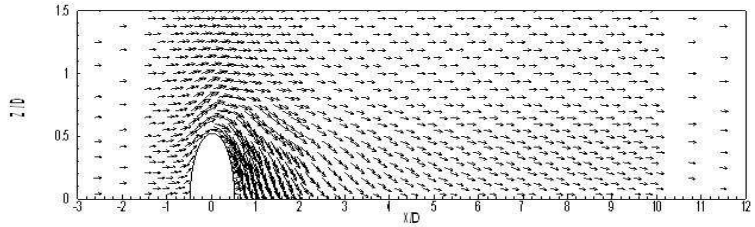

Fig. 6: The velocity vectors in the lateral plane (X/D, Z/D) at Y/D ≈0

The Figure 7 shows the velocity vectors plotted from $\tilde{U}$ and $\tilde{V}$ in the longitudinal planes (X,Y) for Z/D = 0, -0.25, -0.5, and -0.75, compared with experimental results. These representations perform a global survey on importance of the boundary layer region disturbed by the jet not far more than 1D in height, less than 20D long

and -0.75D large. The comparison with experimental results shows generally good agreement according to the four longitudinal planes. However, at Z/D = 0 and Z/D = - 0.25, experimental results show that the flow is turned down towards the wall ($\tilde{V} < 0$) ranging from 1 to 2 while calculated results do not show this turndown ($\tilde{V} > 0$). This behaviour is not reproduced by the turbulence model.

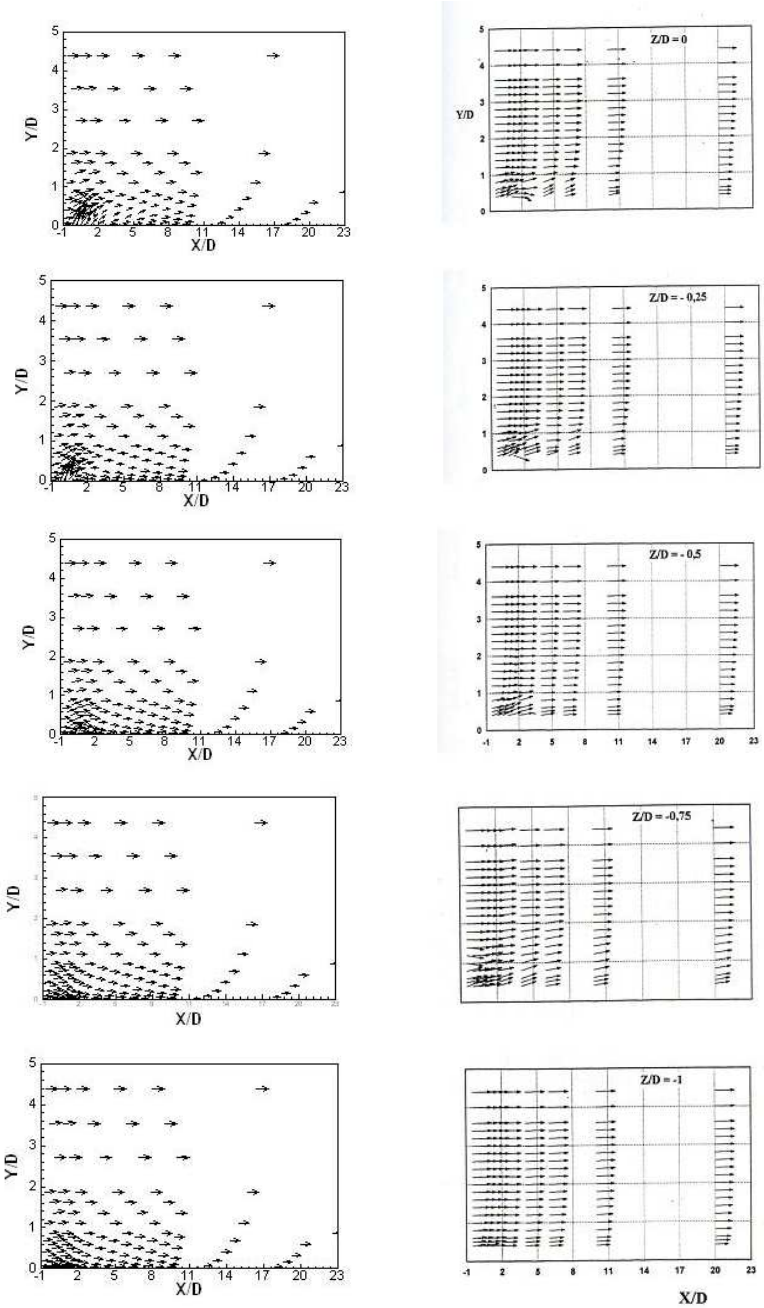

Fig. 7: The velocity vectors plotted in the longitudinal planes (X/D,Y/D)
(Experiments on right side, calculation on left side)

The spreading-temperature may be improved by presenting the data in the form of constant dimensionless temperature at a centerline plane normal to the surface plate. Values of constant temperature contours are presented in Figure 8 at Z/D = 0. The maximum temperatures occur at a position Y/D = 0.5 above the wall and between X/D=-1 and X/D = 4. As the jet travels downstream, it spreads in such a way that the location of maximum temperature moves closer to the wall. Confrontation with experimental data along the centerline shows that the jet penetration and the vertical spreading are predicted around the jet (X/D = 4). Beyond X/D = 4, the calculated thermal plume quickly joined the wall compared with the experimental results, one observes a fast turbulent diffusion of heat. At the axial distances of X/D = 2 to X/D = 14, the predicted constant temperature contours is in good agreement with the experimental results obtained above the wall.

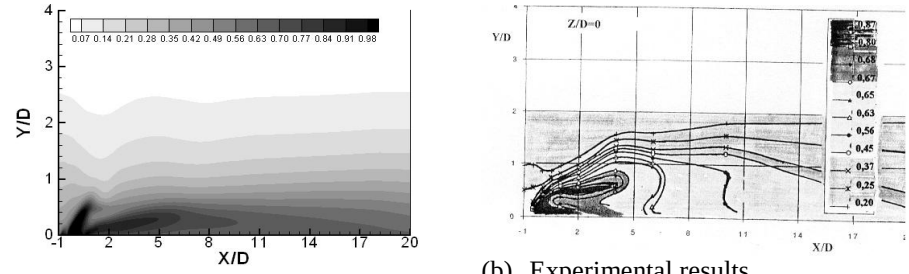

(a) Numerical results (b) Experimental results

Fig. 8: Constant temperature contours profiles

This general survey of temperature evolution is also presented in Figure 9 according to horizontal planes for Z/D = - 0.25,-0.5,-0.75 and 1.The thermal diffusion of the jet extends at -0.75D. The jet is diffused to height reaching 0.5D for Z/D = - 0.25 and Z/D = - 0.5. The hot jet spray begins eases beyond Z/D = - 0.75.

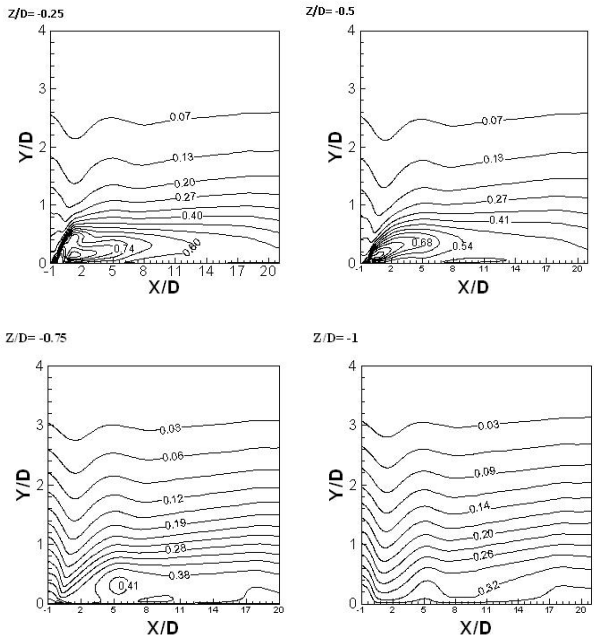

Fig. 9: Temperature evolution in horizontal planes (X/D,Y/D).

Conclusions:

The numerical results are assessed through comparisons with experimental measurements. It was found, in general that the jet centreline and the wake region can be predicted with an optimal number of grid points (164×90×31). However, a discrepancy was demonstrated between the computation and the experiment especially for the wake strength. The influence of the injection is better made into evidence upstream and in the vicinity of the injection zone. The disturbance is deadened more quickly and the wake zone is averagely presented in the calculated profiles. The temperature profiles are badly predicted in the wake zone, this can be due to the isotropic simple eddy diffusivity model based on the Boussinesq approximation where the Prandtl number chosen in our calculation is 0.9.

REFERENCES

Baheri, S., S.P. Alavi Tabrizi and A. Jubran, 2008. Film cooling effectiveness from trenched shaped and compound Holes.' Heat Mass Transfer, 44(8): 989-998.

Baldauf, S., A. Schulz and S. Wittig, 1999 *High resolution measurements of local heat transfer coefficients by discrete hole film cooling*.' ASME pp: 99-GT-43.

Bayraktar, S. and T. Yılmaz, 2011. Three-dimensional analysis of temperature field for various parameters affect the film cooling effectiveness. Energy Conversion and Management, 52: 1914-1929.

Dizene, R., J.M. Charbonnier, E. Dorignac and R. Leblanc, 2000. Etude expérimentale d'une interaction de jets obliques avec un écoulement transversal compressible. I. Effets de la compressibilité en régime subsonique sur les champs aérothermique. Int. J. Therm. Sci., 39(3): 390-403.

Dizene, R., J.M. Charbonnier, E. Dorignac and R. Leblanc, 2000. Etude expérimentale d'une interaction de jets obliques avec un écoulement transversal compressible. II. Effets du taux d'injection sur les transferts thermiques en surface. Int. J. Therm. Sci., 39(5): 571-581.

Gatski, T.B. and C.G. Speziale, 1993. On explicit algebraic stress models for complex turbulent flow. J. Fluid. Mech., 254: 59-78.

Guo, X., W. Schroder and M. Meinke, 2006. Large-eddy simulations of film cooling flows. Computers and Fluids, 35(6): 587-607.

Hahn, S. and H. Choi, 1997. Unsteady simulation of jets in a cross- flow. J. Comput. Phys., 134(2): 342-56.

Hoda, A. and S. Acharya, 2000. Predictions of a film coolant jet in cross-flow with different turbulence models. ASME J. Turbomach,, 122(3): 558-569.

Launder, B.E. and D.B. Spalding, 1974. The numerical computation of turbulent flows. Comp. Meth. App. Mech. Eng., 3(2): 269-289.

Patankar, S.V., 1980. *Numerical Heat Transfer and fluid flow*, McGraw Hill.

Pope, S.B., 1975. A more general effective viscosity hypothesis. J. Fluid. Mech., 72(2): 331-340.

Rumsey, C.L., T.B. Gatski and J.H. Morrison, 2000. Turbulence model predictions of strongly curved flow in u-duct. AIAA Journal., 38: 394-1402.

Speziale, C.G., S. Sarkar and T.B. Gatski, 1991. Modeling the pressure-strain correlation of turbulence: an invariant dynamical systems approach. J. Fluid. Mech., 227(1): 245-272.

Tyagi, M. and S. Acharya, 2003. Large eddy simulation of film cooling flow from an inclined cylindrical jet. J. of Turbomachinery, 125(4): 734-742.